Experimental Demonstration of the Stability of Berry's Phase for a Spin-1/2 Particle

S. Filipp,[1,2,3,*] J. Klepp,[1,3] Y. Hasegawa,[1] C. Plonka-Spehr,[3] U. Schmidt,[4] P. Geltenbort,[3] and H. Rauch[1]

[1]*Atominstitut der Österreichischen Universitäten, Stadionallee 2, A-1020 Vienna, Austria*
[2]*Department of Physics, ETH Zurich, CH-8093 Zürich, Switzerland*
[3]*Institut Laue Langevin, Boîte Postale 156, F-38042 Grenoble Cedex 9, France*
[4]*Physikalisches Institut, Philosophenweg 12, 69120 Heidelberg, Germany*
(Received 25 August 2008; published 22 January 2009)

The geometric phase has been proposed as a candidate for noise resilient coherent manipulation of fragile quantum systems. Since it is determined only by the path of the quantum state, the presence of noise fluctuations affects the geometric phase in a different way than the dynamical phase. We have experimentally tested the robustness of Berry's geometric phase for spin-1/2 particles in a cyclically varying magnetic field. Using trapped polarized ultracold neutrons, it is demonstrated that the geometric phase contributions to dephasing due to adiabatic field fluctuations vanish for long evolution times.

DOI: 10.1103/PhysRevLett.102.030404 PACS numbers: 03.65.Vf, 03.65.Yz, 03.75.Be

The rapidly increasing capability to control and measure quantum states on a single particle level (see, e.g., [1] and references therein) demands for decoherence free systems and robust manipulation techniques. In order to enable high-precision quantum measurements [2] or quantum information processing [3], a system should be decoupled from the environment except for precisely controllable interactions. As part of the quest for reliable quantum gates, the *geometric phase* has attracted renewed attention due to its potential resilience against noise perturbations.

In short, the adiabatic evolution of a quantum system returning after some time to its initial state gives rise to an additional phase factor, termed Berry phase [4]. The peculiarity of this phase lies in the fact that its magnitude is not determined by the dynamics of the system, i.e., neither by energy nor by evolution time, but purely by the evolution path from the initial to the final state. A vast number of experiments have verified its characteristics in various systems [5]. Several extensions, for instance to nonadiabatic, noncyclic, nonunitary, or non-Abelian geometric phases have been investigated [6]. For closed quantum systems, the geometric phase is theoretically well understood and experimentally verified. However, for open quantum systems, the situation is different in that no general framework has found approval yet. Concepts of geometric phases for mixed state evolutions have been introduced theoretically [7–9] and inspected experimentally [10–13]. Also dephasing induced by the geometric phase has been studied theoretically for several settings [14–17]. Potential advantages of geometric quantum gates for quantum information processing have been a topic of recent investigation [18–20]. Furthermore, high-fidelity geometric gates are currently used in ion traps [21] suggesting Berry's adiabatic geometric phase as a favorable choice for quantum state manipulations. In [22], it is calculated that the contribution of the geometric phase to dephasing are path-dependent like the geometric phase itself and that they diminish for long evolution times.

In this Letter, we consider the situation of an adiabatic evolution of a spin-1/2 system and explicitly test the influence of slow fluctuations onto the Berry phase. By analyzing the influence of evolution time on the geometric dephasing using an ultracold neutrons setup [23], we show that the Berry phase is robust against adiabatic fluctuations in the driving field, when the evolution time is longer than the typical noise correlation time.

Consider a spin-1/2 particle exposed to slowly varying magnetic fields. The Hamiltonian

$$H(t) = -\mu\vec{\sigma}\cdot\vec{B}(t) = -\mu[\vec{\sigma}\cdot\vec{B}_0(t) + \sigma_x K(t)] \quad (1)$$

describes the coupling of a particle to the magnetic field $\vec{B}(t)$ by its spin magnetic moment μ. The magnetic field has magnitude $B(t) \equiv |\vec{B}(t)|$, and its direction points along the unit vector $\vec{n}(t) = [\cos\vartheta(t), \sin\vartheta(t)\sin\varphi(t), \sin\vartheta(t)\times\cos\varphi(t)]^T$. $\vec{\sigma} = [\sigma_x, \sigma_y, \sigma_z]^T$ denote the Pauli matrices and $K(t)$ stands for an additional fluctuating magnetic field along the x-axis. Let $|s_\pm(t)\rangle$ denote the time-dependent spin eigenstates of $H(t)$. If the system is initially in an eigenstate $|s_\pm(0)\rangle$, it will stay in an eigenstate during an adiabatic evolution of the B-field. In other words, the B-field direction and the polarization vector of the particles' spin $\vec{s}(t)$ coincide for all times, where $\vec{s}(t) \equiv \mathrm{Tr}[\vec{\sigma}\cdot\rho(t)]$ for the system being in the state described by the density matrix $\rho(t)$. In spherical coordinates,

$$\vec{s}(t) = s[\cos\theta(t), \sin\theta(t)\sin\phi(t), \sin\theta(t)\cos\phi(t)]^T. \quad (2)$$

Its length $s \equiv |\vec{s}|$ represents the degree of polarization. For a pure state $\rho(t) = |s_\pm(t)\rangle\langle s_\pm(t)|$, we have $s = 1$, but in general, interactions with the environment lead to mixed states with reduced $s < 1$ as discussed below.

Within the adiabatic approximation, where $\theta(t) \approx \vartheta(t)$ and $\phi(t) \approx \varphi(t)$, a cyclic variation of the B-field coordinates $\vartheta(t)$ and $\varphi(t)$ leads only to a change of the phase of the initial state $|s_\pm(0)\rangle$ after the evolution. The final state $|s_\pm(T)\rangle = e^{\pm i(\phi_g+\phi_d)}|s_\pm(0)\rangle$ comprises a dynamical (ϕ_d) and a geometric (ϕ_g) phase. $\phi_d = -\int_0^T E(t)dt/\hbar$ is determined by the integrated instantaneous energies $E(t) = -\mu\langle s_\pm(t)|\vec{\sigma}\cdot\vec{B}(t)|s_\pm(t)\rangle$. It depends explicitly on the dynamics of the state transport. In contrast, the geometric phase ϕ_g is determined only by the solid angle Ω enclosed by the path of the state: $\phi_g = -\Omega/2$ for a spin-1/2 particle. It is independent of energy and time. In particular, the B-field we have used in our experiment traces out a path with constant ϑ and varying $\varphi(t) \in [0, 2\pi]$. Without fluctuations $[K(t) = 0]$, the geometric phase evaluates to $\phi_g^0 \equiv -\pi(1 - \cos\vartheta)$.

Field fluctuations in x-direction during the evolution are represented by the term $\sigma_x K(t)$ (with equivalent results holding also for isotropic noise involving $\sigma_{z,y}$ terms [22]). Fluctuations in the Larmor frequency $\omega_L = 2\mu B/\hbar$ are then given by $2\mu K(t)/\hbar$, which denotes a Gaussian and Markovian noise process with intensity σ_P^2 and correlation time $1/\Gamma$, i.e., noise bandwidth Γ. We assume an upper cutoff frequency of the noise $\Gamma_{\max} \ll \omega_L$ such that the field fluctuations are adiabatic with respect to the Larmor frequency. Later in the experiment, this is achieved by adding adequately designed noise to the field. Consequently, the variations in the path, and therefore in Ω, lead to variations in the geometric phase. The random geometric phase ϕ_g is Gaussian distributed with mean value equal to the noise-free case, $\langle\phi_g\rangle = \phi_g^0$. Its variance $\sigma_g^2(T)$ depends on the evolution time T and is given by [22]

$$\sigma_{\phi g}^2(T) = 2\sigma_P^2\left(\frac{\pi\sin^2\vartheta}{T\omega_L}\right)^2\left[\frac{\Gamma T - 1 + e^{-\Gamma T}}{\Gamma^2}\right]. \tag{3}$$

The dependence on the factor $\sin^2\vartheta$ has been tested in [24]. A further intriguing property is that for evolutions, which are slow relative to the noise fluctuations ($T \gg 1/\Gamma$), the variance of the geometric phase drops to zero for long evolution times as the expression in Eq. (3) reduces to $\sigma_{\phi g}^2(T) \propto \frac{1}{T}$ [25]. This contrasts the behavior of the variance of the dynamical phase that increases linearly in time.

In our experiment, we have used neutrons as a precisely manipulable spin-1/2 quantum system. Exposure to a magnetic field leads to Zeeman-energy splitting of $2\mu_n B$ with $\mu_n = -9.66 \times 10^{-27}$ J T^{-1}. The experimental setup is shown in Fig. 1 and more details can be found in [23]. Neutrons are guided from the ultracold neutron source at the ILL high flux reactor through magnetized Fe polarization foils, which give a degree of polarization of about 90%, to the storage bottle (filling). Their low kinetic energy prohibits penetration through the walls of the bottle. During a typical storage time of 10 s, the spin orientation of the dilute (≈ 1 neutron/cm^3) gas of practically noninteracting spin-1/2 particles can be arbitrarily manipulated by magnetic fields produced by a 3D Helmholtz-coil setup (manipulation). The resulting spin polarization is subsequently analyzed by a combination of a fast adiabatic π-flipper ($\approx$99% efficiency) and the polarization foils before hitting the detector (emptying). A full storage cycle of filling, manipulation, and emptying lasts about 70 s.

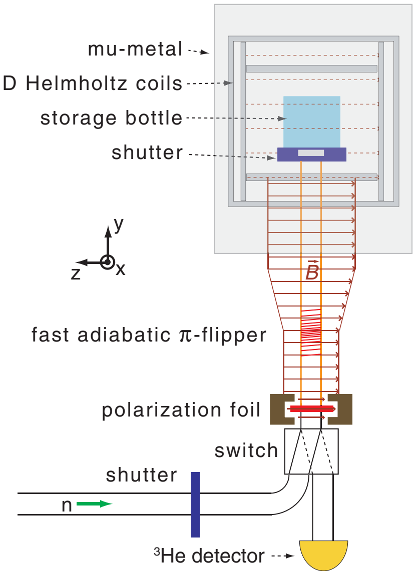

FIG. 1 (color online). Experimental setup, see text.

Here, we focus on the manipulation stage: First, we have compared the initial to the final polarization after a cyclic variation of the magnetic guide field $[\vec{B}(0) = \vec{B}(T)]$ with the neutron spin initially aligned with the static magnetic guide field in the negative z-direction. To find identical initial and final polarization, the adiabaticity condition requires a rate of change of the B-field much smaller than the Larmor frequency ω_L of the system. Within the accuracy of the experiment, this applies for a typical rate of change less than $\approx 0.2\omega_L$, which sets the upper limit for the following measurements.

Second, a Ramsey-type interferometric scheme similar to [27] has been employed for the measurement of Berry's phase. As shown in Fig. 2, the actual evolution of the B-field is preceded by a $\pi/2$-pulse induced by a rf-field in x-direction with amplitude 1.6 μT, duration 10.7 ms and a frequency resonant with the magnetic guide field $B_z(0) = -10$ μT. Starting from the eigenstate $|s_+(0)\rangle$, this generates an equal superposition of spin-up and spin-down states, $|\psi(0)\rangle = [|s_+(0)\rangle + |s_-(0)\rangle]/\sqrt{2}$. A subsequent adiabatic and cyclic B-field evolution of duration T induces a relative phase between the states of $\phi(T) = \phi_g + \phi_d$. The resulting spin polarization $\vec{s}(T)$ can be analyzed by $\pi/2$-pulses, which are offset in phase by zero or 90° relative to the preparatory $\pi/2$-pulse. A further π-flip can be induced with high efficiency by the subsequent fast adiabatic π-flipper. Together with the final projective measurement along the positive z-direction, this gives a complete set of measurements of the $\pm x$, $\pm y$ and $\pm z$ polarization components. In this way, the final spin state is characterized with an efficiency close to 100%. The initial degree of polarization $s_0 \equiv |\vec{s}(0)|$ is typically 75%. During the evolution, s_0 is reduced mainly due to static field inhomogeneities across the storage volume—even without temporal fluctuations, i.e., for $K(t) = 0$ [23]. Local variations in the B-field magnitude cause variations

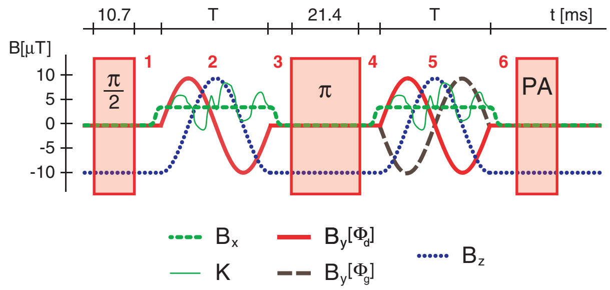

FIG. 2 (color online). Pulses for the B-field (x- y- and z-direction) for measuring the geometric phase: A $\pi/2$-pulse is followed by a cyclic B-field evolution. A subsequent π-pulse flips the spin such that the preceding evolution can be compensated ($B_y[\phi_d]$). The resulting spin state is determined by the polarization analysis (PA). Measuring the geometric phase ϕ_g involves a change of the rotation direction while keeping the magnitude fixed ($B_y[\phi_g]$). Identical fluctuations are generated in x-direction (K) for measuring geometric dephasing.

in the Zeeman-energy splitting. Consequently, the relative phases in the final spin superposition states of the individual neutrons are randomly distributed, which leads—on average—to dephasing. This causes a further loss of polarization $s(T) = s_0 e^{-T/T_2}$. $T_2 = 847(40)$ ms has been measured by a polarization analysis after free precession of the spin superposition state in a 10 μT magnetic field. This sufficiently exceeds typical evolution times of 500 ms.

To measure the geometric phase $\phi_g^0 = -\Omega/2$ for $K(t) = 0$, the magnetic guide field pointing initially in the negative z-direction is rotated about the x-axis, i.e., $B_y(t) = -B_z(0)\sin(\omega t)$ and $B_z = B_z(0)\cos(\omega t)$ with constant $|\vec{B}(t)|$ (see Fig. 2). An additional offset field B_x in x-direction generates a conical section traced out by the magnetic field vector and—in the adiabatic limit—also by the spin polarization vector. The enclosed solid angle $\Omega = \pi(1 - \cos\vartheta)$ is determined by the cone angle $\vartheta = \tan^{-1}B_z/B_x$. To eliminate contributions from the dynamical phase ϕ_d, we invoke a spin-echo scheme [28,29]. The according evolution path of the spin-up component $\vec{s}^+(t) \equiv \mathrm{Tr}[\vec{\sigma}|s_+(t)\rangle\langle s_+(t)|]$ of the superposition state on the Bloch-sphere is illustrated in Fig. 3(a). Depending on the rotation direction, the solid angle enclosed by the path on the lower hemisphere $\Omega_{SE} = \pm\Omega$. Thus, if the direction of rotation is reversed after a π-pulse and the field amplitude is kept constant, the geometric phase doubles—due to its dependence on the directed solid angle—while the dynamical phase cancels. Both the accumulation of the geometric phase and the cancellation of the dynamical phase has been measured using the pulse sequence drawn in Fig. 2 for $T = 200$ ms. The solid angle Ω is varied by choosing different B_x offset fields. The ratio $\omega/\omega_L = 2\pi/(T\omega_L) \approx 0.017$ ensures adiabaticity of the evolution. In Fig. 3(b), the measured geometric phase ϕ_g is plotted as a function of Ω. The fit to the measured data yields $\phi_g^0 = -0.51(1)\ \Omega$ which is in good agreement with the expected $\phi_g^0 = -\Omega/2$. Residual dynamical phase contributions, which are not compensated by the spin echo, are measured to be 0.22 rad. These are determined by the phase difference in the final polarization between the spin-echo with identical evolution (Fig. 2 for $B_y[\phi_d]$) and without evolution at all [$B_z(t) = \text{const}$, $B_x(t) = B_y(t) = 0$].

For testing the stability of the geometric phase, we generate field fluctuations $K(t)$ [c.f. Eq. (1)] with Lorentzian power spectrum [26], a bandwidth of $\Gamma = 100\ \mathrm{rad\,s^{-1}}$ and intensity $\sigma_P^2 = 4\ \mu\mathrm{T}^2$ as the mean square deviation of the fluctuations. We apply a smooth rectangular-shaped window function to the noise in the time-domain to avoid nonadiabatic and noncyclic effects. To test the time dependence of the variance of the geometric phase $\sigma_{\phi g}^2(T)$ given by Eq. (3), the evolution time T is changed from $T = 35$ ms to $T = 250$ ms. The different fluctuations in subsequent storage cycles lead to different phases ϕ of the final state. But since the noise is identical for both first and second part of the spin-echo, these difference can only originate in the geometric phase. The dynamical phase cancels as before in the fluctuation-free measurements. The average over several storage cycles, i.e., several noise patterns, gives a further shrinking of the length of the polarization vector $s(T)$ of the final state additional to the unavoidable polarization losses discussed above: In fact, for Gaussian distributed ϕ, we obtain $\langle\cos\phi\rangle = \exp[-\sigma_\phi^2/2]\cos\langle\phi\rangle$ in Eq. (2). Consequently, the purely geometric dephasing gives $s_n(T) = s(T) \times \exp\{-[4\sigma_{\phi g}(T)]^2/2\}$, where the factor 4 is due to the particular type of measurement [30] and small fluctuations in θ are neglected. To separate the unavoidable polarization losses from the geometric dephasing, the geometric phase has been measured with and without fluctuations and the ratio of the corresponding degrees of polarization

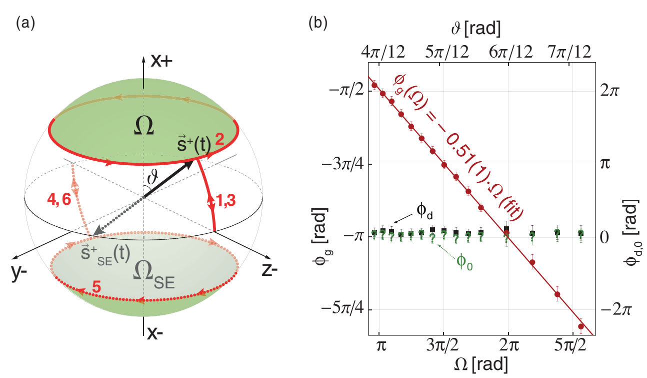

FIG. 3 (color online). (a) Path traced out by the spin-up state $\vec{s}^+(t)$ on the Bloch-Sphere while following the adiabatic changes in the magnetic field. After the first cycle (path 1-2-3), the state vector is flipped ($\vec{s}^+ \rightarrow \vec{s}^+_{SE}$) and traces out the path 4-5-6 on the lower hemisphere for the second, echo cycle. (b) Measured geometric phase ϕ_g (filled circles). If the sense of rotation is not reversed after the echo pulse, all accumulated phases cancel apart from remaining dynamical contributions ϕ_d (solid rectangles). Ideally, this yields the same phase as if there were no B-field evolution at all (ϕ_0-open circles).

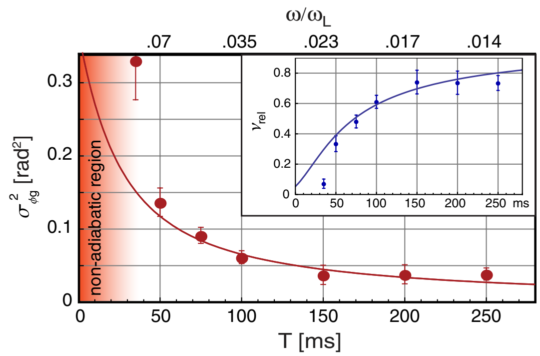

FIG. 4 (color online). The variance $\sigma^2_{\phi g}(T)$ of the geometric phase as a function of the evolution time T in a fluctuating magnetic field. The variance decreases for longer evolution times following closely the theoretical prediction in Eq. (3) (solid line). The inset shows the increase of the degree of polarization ν_{rel} relative to the noise-free evolution.

$\nu_{\mathrm{rel}}(T) \equiv s_n(T)/s(T)$ gives the variance of the geometric phase $\sigma^2_{\phi g}$. For each value of T, 300 different noise realizations have been performed, where a sequence of six storage cycles forms the polarization analysis. In Fig. 4, we have plotted the decrease of $\sigma^2_{\phi g}$ as a function of the evolution time T and fixed noise-free geometric phase $\phi_g^0 = -2.56$ rad. The inset shows the corresponding increase in the relative degree of polarization ν_{rel}. Error bars stem from the limited number of noise realizations. The solid line indicates the theoretical predictions given by Eq. (3) for the adjusted experimental parameters without free parameters. Because of the low-pass filtering of the coils and nonadiabatic corrections, the datapoint at $T = 35$ ms deviates from the theory curve by 3σ. We have also verified that the mean geometric phase remains unaffected: $|\langle\bar{\phi}_g\rangle - \phi_g^0| = 0 \pm 0.1$ rad, where $\langle\bar{\phi}_g\rangle$ denotes the geometric phase averaged over the different values of T.

In summary, we have measured the stability of the adiabatic geometric phase with respect to magnetic field fluctuations as a function of evolution time. A spin-echo technique allowed for the observation of the purely geometric part of the dephasing of the quantum state. The acquired data show very good agreement with theoretical predictions and demonstrate the vanishing influence of geometric dephasing for slow evolutions. Clearly, when considering quantum gates, a compromise has to be found between the superior noise resilience but slower execution speed compared to dynamical phase gates. In this context, generalized settings involving nonadiabatic geometric phases [31] provide an interesting perspective for future experimental efforts. In the adiabatic regime, the results presented above demonstrate that the geometric phase can indeed be useful for high-fidelity quantum state manipulations.

This work was supported by the Austrian Science Foundation (FWF) and the Japan Science and Technology Agency (JST). The authors want to thank K. Durstberger, E. Sjöqvist, S. Sponar, and R. Whitney, as well as R. Loidl, P. Pataki, E. Tischler, and T. Brenner for valuable discussions and for technical assistance.

*filipp@phys.ethz.ch

[1] S. Haroche and J.-M. Raimond, *Exploring the Quantum* (Oxford Univ. Press, Oxford, 2006).
[2] C. F. Roos *et al.*, Nature (London) **443**, 316 (2006).
[3] M. A. Nielsen and I. L. Chuang, *Quantum Computation and Quantum Information* (Cambridge University Press, Cambridge, United Kingdom, 2000).
[4] M. V. Berry, Proc. R. Soc. A **392**, 45 (1984).
[5] *Geometric Phases in Physics* edited by A. Shapere and F. Wilczek (World Scientific, Singapore, 1989).
[6] Y. Aharonov and J. Anandan, Phys. Rev. Lett. **58**, 1593 (1987); J. Samuel and R. Bhandari, Phys. Rev. Lett. **60**, 2339 (1988); D. M. Tong, E. Sjöqvist, L. C. Kwek, and C. H. Oh, Phys. Rev. Lett. **93**, 080405 (2004); F. Wilczek and A. Zee, Phys. Rev. Lett. **52**, 2111 (1984).
[7] E. Sjöqvist *et al.*, Phys. Rev. Lett. **85**, 2845 (2000).
[8] A. Uhlmann, J. Geom. Phys. **18**, 76 (1996).
[9] M. Ericsson *et al.*, Phys. Rev. Lett. **91**, 090405 (2003).
[10] J. Du *et al.*, Phys. Rev. Lett. **91**, 100403 (2003).
[11] M. Ericsson *et al.*, Phys. Rev. Lett. **94**, 050401 (2005).
[12] J. Du *et al.*, arXiv:0710.5804v1.
[13] J. Klepp *et al.*, Phys. Rev. Lett. **101**, 150404 (2008).
[14] A. Blais and A. M. S. Tremblay, Phys. Rev. A **67**, 012308 (2003).
[15] M. S. Sarandy and D. A. Lidar, Phys. Rev. A **73**, 062101 (2006).
[16] R. S. Whitney, Y. Makhlin, A. Shnirman, and Y. Gefen, Phys. Rev. Lett. **94**, 070407 (2005);R. S. Whitney and Y. Gefen, Phys. Rev. Lett. **90**, 190402 (2003).
[17] I. Fuentes-Guridi, F. Girelli, and E. Livine, Phys. Rev. Lett. **94**, 020503 (2005).
[18] P. Zanardi and M. Rasetti, Phys. Lett. A **264**, 94 (1999).
[19] J. A. Jones, V. Vedral, A. Ekert, and G. Castagnoli, Nature (London) **403**, 869 (2000).
[20] G. Falci *et al.*, Nature (London) **407**, 355 (2000).
[21] D. Leibfried *et al.*, Nature (London) **422**, 412 (2003).
[22] G. DeChiara and G. M. Palma, Phys. Rev. Lett. **91**, 090404 (2003).
[23] S. Filipp *et al.*, Nucl. Instrum. Methods Phys. Res., Sect. A **598**, 571 (2009).
[24] P. J. Leek *et al.*, Science **318**, 1889 (2007).
[25] A more general theory predicts a renormalized geometric phase and a finite time-scale of the decrease [15,16,26].
[26] S. Filipp, Eur. J. Phys. Special Topics **160**, 165 (2008).
[27] D. J. Richardson, A. I. Kilvington, K. Green, and S. K. Lamoreaux, Phys. Rev. Lett. **61**, 2030 (1988).
[28] A. Abragam, *Principles of Nuclear Magnetism* (Oxford Univ. Press, Oxford, United Kingdom, 1961).
[29] R. A. Bertlmann, K. Durstberger, Y. Hasegawa, and B. C. Hiesmayr, Phys. Rev. A **69**, 032112 (2004).
[30] Both the preparation of a superposition state and the spin-echo give a factor of 2 for the phase.
[31] S.-L. Zhu and P. Zanardi, Phys. Rev. A **72**, 020301(R) (2005).